Disease Prevention and Epidemiology

https://dpe.cultechpub.com/dpe

Cultech Publishing

Review

Designing Multi-Epitope mRNA Vaccine Models Against Yezo Virus by Screening the Whole Proteome Using Immunoinformatics Approaches

Awais Ali[1,*], Shahid Nawab[1], Muhammad Fawad[2]

[1]Department of Biochemistry, Abdul Wali Khan University Mardan, Mardan, Pakistan

[2]Department of zoology Islamia college Peshawar, Peshawar, Pakistan

[*]Corresponding author: Awais Ali, awaisalibio@gmail.com

Abstract

Yezo virus (YEZV), a recent discovery among emerging human pathogens associated with public health burden and causes acute febrile illness, thrombocytopenia, and leukopenia. Currently, no vaccine is available on the market against YEZV infection. The current study based on the prediction of a novel mRNA vaccine design against the YEZV by utilizing whole proteome data. Two Glycoproteins (YP_010840880.1 and YP_010840879.1) were selected based on redundancy removal and homology analysis with the human database. Four model constructs were designed from 18 top-ranked B and T cells overlapped epitopes. The constructs were analyzed based on biophysical and biochemical evaluation. The structural bioinformatics analysis predicted good quality and stable 3D structures for the designed constructs. Molecular docking and Molecular dynamic simulation analyses prioritized the YEZV-V2 model to interact and exhibited the highest binding affinity with the HLA and TLRs immune receptors. The immune simulation analysis predicted YEZV-V2's ability to enhance both cellular and humoral immune responses in humans. Finally, the Prioritized YEZV-V2 vaccine model was modified into circular RNA with helper sequences to enhance its circulation and translation, aiming to establish its effectiveness against the YEZV. However, experimental and clinical follow-up of these *In-silico* investigations may be required for designed mRNA vaccine.

Keywords

mRNA vaccine model, Thrombocytopenia, Yezo virus, Reverse vaccinology, Immuno-informatics

Article History

Received: 17 December 2025
Revised: 29 January 2026
Accepted: 26 February 2026
Available Online: 28 February 2026

Graphical Abstract

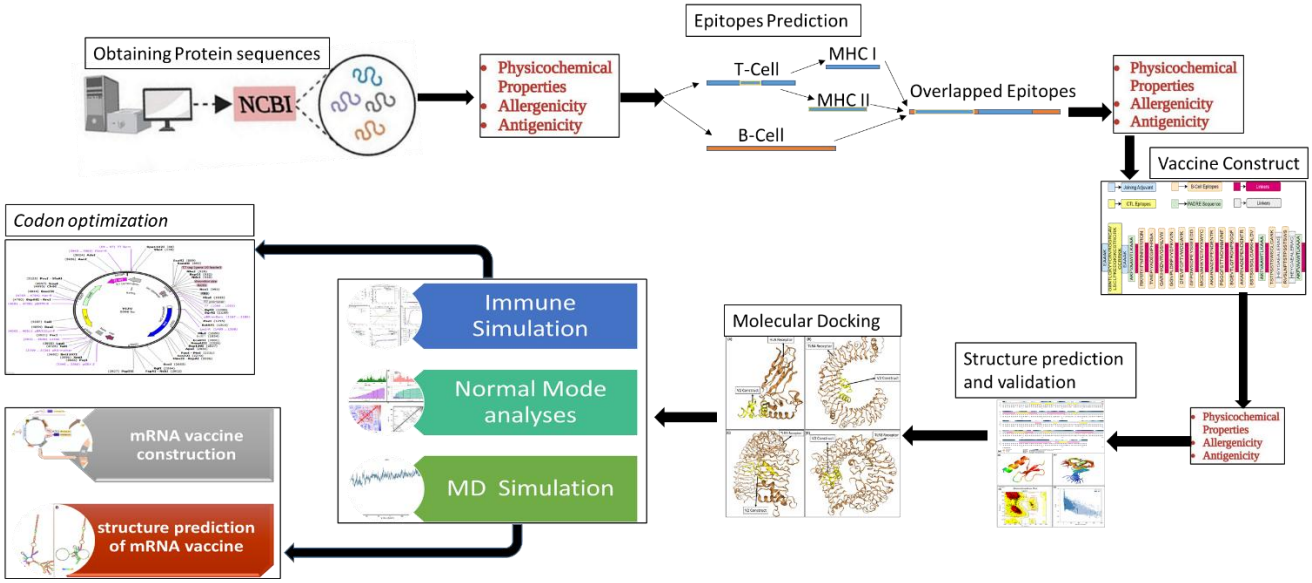

1. Introduction

The Yezo virus (YEZV) is a recently identified tick-borne pathogen belonging to the *Sulina genogroup* within the genus *Orthonairovirus*, family *Nairoviridae*. It was first discovered in Japan, where nine confirmed human cases were reported between 2014 and 2020, and one additional case was documented in China in 2018 [1-3]. YEZV is transmitted through tick bites, and its RNA has been detected in several tick species, suggesting a zoonotic transmission cycle between arthropods and mammalian hosts. Clinically, YEZV infection manifests as an acute febrile illness accompanied by leukopenia and thrombocytopenia, along with symptoms such as fatigue, nausea, chest pain, and visual disturbances [4,5] Although YEZV infections remain rare and geographically confined to East Asia, its detection in multiple tick vectors and serological evidence of exposure in wild mammals indicate a potential for broader ecological circulation. While current data do not support a significant increase in human cases or widespread transmission, early research into preventive strategies is warranted to mitigate potential future spillover events [4,6].

From a virological standpoint, YEZV shares close genetic and structural similarity with other members of the Orthonairovirus genus, particularly Crimean Congo hemorrhagic fever virus (CCHFV) and Dugbe virus (DUGV). Like its relatives, YEZV possesses a tripartite negative-sense RNA genome encoding the nucleoprotein (N), glycoprotein precursor (GPC), and RNA-dependent RNA polymerase (L). The GPC, which undergoes cleavage into Gn and Gc glycoproteins, facilitates viral entry into vascular endothelial and hepatic cells, reflecting YEZV's tropism for vascular and hepatic tissues. The N protein functions as a major virulence determinant by suppressing type I interferon signaling and sequestering viral double-stranded RNA, thereby inhibiting early antiviral responses. The mRNA-based vaccines have proven remarkably effective strategy to prevent and eradicate infectious diseases throughout the history of mankind due to rapid development capacity, their high potency, safe administration, and low-cost manufacturing. Vaccination is particularly worthy for low-income individuals with limited access to healthcare [7]. Several immunoinformatics-based studies have proposed multi-epitope vaccine (MEV) constructs for YEZV and related orthonairoviruses [6,8-10]. however, these reports largely emphasize peptide or protein subunit approaches, without addressing RNA-level optimization critical for *in vivo* translation efficiency and stability. In contrast, the present study integrates a comprehensive immunoinformatics pipeline with mRNA-specific design principles, including (1) full-proteome antigen screening to identify non-redundant and non-paralogous vaccine targets, (2) multi-epitope assembly based on antigenicity, non-allergenicity, and host-homology exclusion, and (3) RNA-level optimization of codon usage and secondary structure prediction using the Java Codon Adaptation Tool (JCAT) and RNAfold [11]. Messenger RNA (mRNA)-based vaccines have recently transformed vaccine development due to their high potency, rapid scalability, and safety profile[12-14]. However, their low immunogenicity remains a significant challenge [15,16]. Recently, circular RNA (circRNA) vaccine technology has emerged as a novel alternative to traditional linear mRNA vaccines. Unlike linear mRNA, circRNAs form covalently closed loops that lack free 5′ and 3′ ends, rendering them highly resistant to exonuclease degradation and potentially capable of sustained antigen expression [17-19]. These properties make circRNAs an attractive exploratory platform for vaccine development. However, the immunogenic and translational advantages of circRNAs over conventional mRNA vaccines remain largely theoretical and require experimental validation. Therefore, in this study, we present a computational framework for designing a circular mRNA

(circRNA) MEV against YEZV as a *hypothesis-driven extension* of immunoinformatics-based vaccine design, providing a foundation for future *in vitro* and *in vivo* evaluation.

In this research, our main objective was to identify and design potential mRNA vaccine targets within the YEZV proteome. To achieve this, we utilized non-redundant and non-paralogous human sequence homology, along with antigenicity potential, as our selected criteria. Specifically, we focused on predicting T and B cell receptor epitopes that bind to important histocompatibility class MHCI and MHCII, respectively, using the YEZV proteins. As a result, our final vaccine designs comprised a combination of highly antigenic and non-allergenic epitopes derived from these proteins. To validate the designed vaccine's expression, we optimized its mRNA using the JCAT, and RNAfold generated its secondary structure. *In silico* cloning was subsequently performed. The culmination of this work awaits experimental validation to ascertain the safety and efficacy of the vaccine in combating YEZV infections.

2. Methods and Materials

2.1 Proteome Sequence Retrieval

Protein sequence for YEZV was retrieved in FASTA format from the NCBI database (Ref: GCF_029888495.1) [20]. To remove redundancy and select non-paralogous sequences, Linux's CD-Hit was used with threshold of 80% similarity filtration and NCBI BLASTp to eliminate homology between protein sequences and human proteins, with the following settings set: e-value cut-off 10% identity 35, query coverage 70%, bit score 100%, and other thresholds are set as default. The ProtParam service calculated the chemical and physical characteristics of the protein sequence. The filtered proteins are then assign Vaxijen V 2.0 (https://www.ddg-pharmfac.net/vaxijen/VaxiJen/VaxiJen.html) with a threshold of 0.4 to determine antigenicity of sequences for antigen prediction [21]. Allertop V 2.0 (https://www.ddg-pharmfac.net/AllerTOP/) was used for Allergenicity predictions [22], while ToxinPred server (https://web.expasy.org/protparam/) for toxicity predictions [23]. The whole flowchart of research is shown in Figure 1.

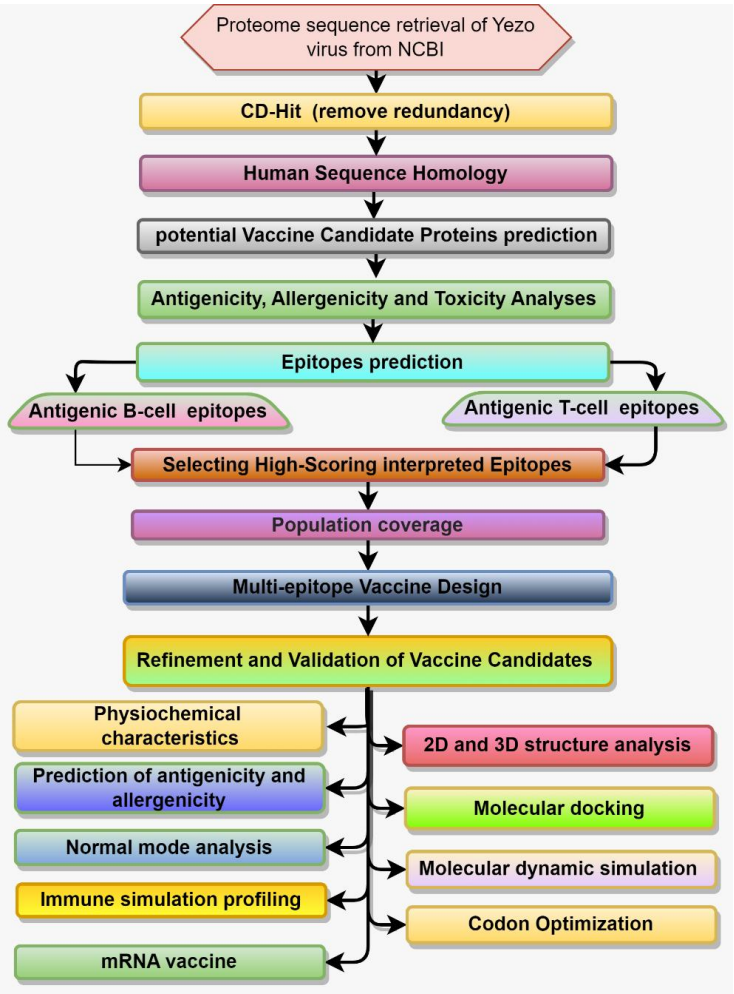

Figure 1. Methodological framework for the construction of a single-subunit MEV against YEZV.

2.2 B and T Cell Epitopes Prediction

T cell epitopes are identified from Immune epitope database (IEDB) by using stabilized matrix method. Further the epitopes are selected by using a threshold of ic50 ≤ 100. Only non-allergenic and nontoxic highly antigenic epitopes are prioritized for further analysis [24]. Due to their ability to elicit a response from the adaptive immune system, B cell epitopes have emerged as fascinating vaccine candidates [25]. For this purpose, the ABCPred software (https://webs.iiitd.edu.in/raghava/abcpred/) was utilized to predict linear B cell epitopes (BCL) [26]. Non-allergen, non-toxic and highly antigenic epitopes are prioritized by using web servers [21,22].

2.3 Conservancy and Population Coverage

The IEDB was implemented to check the conservation and to identify conserved overlapped T and B cell epitopes. All focused were directed on highly conserved epitopes (Table S1). It is vital to take into account the distribution of the HLA genes among various ethnic communities & geographical locations in the creation of a possible vaccine that wants to target a large number of people. Because different populations have different HLA genes, it's important for a vaccine to cover as many people as possible while still functioning within its established norms. We used the population saturation analysis tool (http://tools.iedb.org/population/) hosted on the IEDB AR v.2.22 server to evaluate population coverage of individual epitopes. To estimate the percentage of people who will respond in a given set or epitopes, this tool uses HLA genotypic rates and information on MHC binding with the T cell restriction [27].

2.4 MEV Construction

Glycoproteins of YEZV were selected as vaccine antigens due to their surface accessibility, involvement in viral attachment and entry, and established immunogenicity in enveloped RNA viruses. Selected B cell and T cell epitopes with low percentile ranks, high VaxiJen scores, and confirmed non-allergenic and non-toxic properties were assembled into MEV constructs using appropriate linkers to enhance epitope presentation and prevent junctional epitope formation [28]. Four MEV constructs (V1-V4) were designed by incorporating different immunostimulatory adjuvants, including HBHA , β-defensin [29,30], conserved HBHA, and ribosomal protein adjuvants [31], chosen for their documented roles in enhancing innate immune signaling, antigen processing, and antiviral adaptive immune responses. The EAAAK and GGGS linkers, along with PADRE sequences, were used to ensure structural stability, maintain domain separation, and improve helper T cell activation. This strategy enabled comparative evaluation of adjuvant efficacy within the MEV framework.

2.5 2D and 3D Structure Prediction Validation and Refinement

The PSIPRED v3.3 server (http://bioinf.cs.ucl.ac.uk/psipred), was used to predict the beta-sheet, spirals organization and alpha-helix of the vaccine protein. In order to evaluate PSI-BLAST results, PSIPRED employs two a feed-forward neural systems [32], giving it a dependable and user-friendly platform for 2D homology modeling. The Swiss Model system was employed to anticipate the three-dimensional structures that found in MEV constructions [33]. DeepRefiner, a web server developed by Shuvo et al.,(2021) [34], was used to improve the accuracy of the designed vaccine structures. Additional approaches were used to verify the improved 3D structures of the vaccine constructions. For this, the online structural validation site SAVES v6.0 (https://saves.mbi.ucla.edu/) and its associated ERRAT tool and PROCHECK suite of tools [35,36]. The ProSA-Web Server (https://prosa.services.came.sbg.ac.at/prosa.php) was used for validation [37].

2.6 Determination of Immunological and Physiochemical Properties

Using the Expasy-ProtParam tool (http://www.expasy.org/protparam/), the vaccine sequence was thoroughly examined for a wide range of physicochemical properties. The ProtParam server was used to examine parameters like amino acid composition, protrusion index (PI), half-life, aliphatic score, instability index, molecular weight, and Grand average of hydropathicity (GRAVY) index [38].

2.7 MEV Docking with HLA and TLRs

To ensure effective antigen recognition and immune activation, molecular docking was performed between the designed (MEV and human immune receptors, including HLA class I (PDB ID: 5WJL) and Toll-like receptors TLR3 (PDB ID: 2A0Z), TLR4 (PDB ID: 4G8A), and TLR8 (PDB ID: 3W3M). The HLA alleles were selected based on their global prevalence and immunological significance, with HLA-A02:01, HLA-B07:02, and HLA-DRB101:01* chosen to ensure broad population coverage. The initial docking was performed using the HDock server, followed by refinement of the top complexes using HawkDock, which incorporates protein flexibility in protein-protein docking and employs MM/GBSA scoring for accurate binding energy estimation[39-41]. To verify docking specificity, randomized scrambled peptide controls of equal length and amino acid composition were generated using the ExPASy Random Sequence Generator and

docked to the same receptors. The control peptides exhibited significantly weaker binding affinities (-8.4 to -15.6 kcal/mol) compared to the designed vaccine (-27.9 to -71.3 kcal/mol), confirming interaction specificity [42].

2.8 Normal Mode Analyses and Molecular Dynamic Simulation

Protein mobility and internal flexibility were assessed through normal mode analysis (NMA) using the iMODS web server (https://imods.iqfr.csic.es/) [43]. NMA evaluates collective motions, eigenvalues, and deformability to describe conformational dynamics and molecular adaptability under equilibrium conditions. Further molecular dynamics (MD) simulations were carried out using the Desmond package (Schrödinger LLC) for 150 ns to investigate the dynamic stability of the YEZV-V2-HLA complex [36,44]. The system was solvated in an orthorhombic box with TIP3P water using the OPLS_2005 force field, neutralized with counter ions, and simulated under physiological conditions (300 K, 1 atm, 0.15 M NaCl). The 150 ns simulation window was selected based on prior benchmarking studies in similar immunoinformatics and receptor-ligand systems, where simulations within the 100-500 ns range reliably capture conformational stabilization, hydrogen bonding persistence, and RMSD equilibration trends. Preliminary test runs of 50 ns and 100 ns indicated structural convergence before 120 ns, confirming that 150 ns was sufficient for equilibrium and reproducibility without unnecessary computational overhead. System minimization and equilibration were performed using Maestro's Protein Preparation Wizard. Trajectories were recorded every 100 ps, and stability analyses were based on RMSD and Root Mean Square Fluctuation (RMSF) values [45-47]. The simulations were conducted under constant-volume and temperature ensembles (NVT) to ensure reproducibility. While quantitative variations may occur due to force-field and solvation parameters, the analyses were used as qualitative indicators of stability and relative binding persistence[48,49].

2.9 Immune Simulation

To evaluate the theoretical immune response elicited by the designed vaccine, *in silico* immune simulations were performed using the C-ImmSim v10.1 web server (https://kraken.iac.rm.cnr.it/C-IMMSIM/) [50]. This platform models primary, secondary, and tertiary immune responses based on biological processes involving lymph nodes, bone marrow, and thymic compartments. Simulation parameters were defined as follows: simulation steps = 100, random seed = 12,345, and total doses = 1,000. Common human HLA-binding alleles (A0101, A0201, B0702, B3901, DRB10101, DRB10401) were selected for epitope recognition. The predicted kinetics of antibody titers, cytokine production, and T/B cell populations were analyzed across injection cycles. All results are presented as computational predictions rather than empirical evidence, acknowledging that immune simulation outputs depend on predefined parameters and must be experimentally validated.

2.10 *E. coli* Cloning and Codon Optimization

To ensure optimal expression of the designed vaccine construct in a prokaryotic expression system, codon optimization was performed for the *E. coli* K12 strain. Codon bias between species can significantly affect translation efficiency and protein yield; therefore, the nucleotide sequence of the selected vaccine construct (V2) was optimized using the JCAT (http://www.jcat.de/) [51]. which modifies the nucleotide sequence of the gene to match the host-specific codon usage bias while preserving the original amino acid sequence. During the optimization process, parameters were set to avoid the formation of prokaryotic ribosome binding sites, rho-independent transcription terminators, and restriction enzyme cleavage sites within the sequence. After optimization, restriction sites BglII and ApaI were introduced at the 5′ and 3′ ends, respectively, to facilitate cloning into the pET28a (+) expression vector. The recombinant plasmid design was created using SnapGene software (version 6.0) to ensure the correct orientation and reading frame of the insert within the vector's multiple cloning site. This construct allows for efficient transcription and translation of the target gene under the control of the T7 promoter system in *E. coli* K12 [52].

2.11 mRNA Vaccine Designing

To enhance translation efficiency and ensure stable expression in eukaryotic systems, the designed vaccine sequence was converted into a circRNA construct. The final design was developed based on a modular architecture incorporating functional regulatory and structural elements that facilitate efficient translation, stability, and circularization. The construct design began with the addition of 5′ and 3′ homology arms, which promote autocatalytic circularization of the RNA transcript. Between these termini, a T1 catalytic intron from *T4 phage thymidylate synthase (Td)* was inserted, functioning as a self-splicing element to mediate efficient ligation and circular RNA formation [53]. To enable cap-independent translation, an internal ribosome entry site (IRES) derived from Coxsackievirus B3 (CBV3) was incorporated downstream of the 5′ arm. This ensures ribosome recruitment and initiation in the absence of a 5′ cap, allowing stable translation of the circular construct. A Kozak consensus sequence was also integrated upstream of the start codon to enhance ribosomal recognition. The vaccine coding region contained the optimized signal peptide (tPA) for secretion, an EAAAK linker, and an adjuvant-epitope assembly, reflecting the final arrangement of the vaccine components in the circular RNA precursor. Spacer sequences were strategically inserted to prevent steric hindrance between adjacent domains, ensuring proper RNA

folding and accessibility for ribosomal translation. This comprehensive circRNA design was modeled using SnapGene to visualize the linear-to-circular transformation and validated using the RNAfold web server (ViennaRNA Package 2.0). RNAfold predicted both the minimum free energy (MFE) and centroid structures, confirming the thermodynamic stability of the circular RNA vaccine precursor.The final circRNA vaccine design consisted of the following structural elements in order: 5′ homology arm-T1 catalytic intron-CBV3 IRES-Kozak sequence-tPA-EAAAK linker-adjuvant-epitope assembly-3′ homology arm-Group I PIE sequence.This configuration supports optimal circularization, high translational efficiency, and enhanced RNA stability for the YEZV vaccine construct [54,55].

2.12 Secondary Structure Prediction of the mRNA

The GenSmart codon optimization tool was employed to create an optimized DNA sequence, subsequently converted to an RNA sequence using the DNA > RNA > Protein tool. To predict the secondary structure of the mRNA construct, the RNAfold tool from the ViennaRNA Package 2.0 was utilized [56]. This server provides thermodynamic predictions and assigns a minimal free energy (MFE) score, allowing for the assessment of the MFE structure, centroid secondary structure, and their associated MFE for further analysis. Streamlining this process enhances the efficiency of sequence optimization and structural predictions, facilitating a more comprehensive analysis of the mRNA construct [57,58].

3. Results

3.1 Protein Sequence Retrieval

The whole proteome containing 50 sequences was downloaded from the NCBI database of Yezovirus in FASTA format. three sequences were remained after cutting down redundancy, the CD-Hit database used a sequence similarity criterion of 80%. Antigenicity, non-allergenicity, and toxicity of these proteins were evaluated. Only Two sequences, YP_010840880.1 and YP_010840879.1, were selected after homology analysis towards human proteins database.

3.2 T and B Cell Epitopes Identification and Analysis

The two prioritized proteins are subjected to the IEDB for the prediction of T cell (MHCI and MHCII) epitopes base on the IC50 parameter of <100. The capacity of epitopes to engage with a variety of HLAs and their close connection for binding were key factors in their selection. The ABCPred server predicted the 48 linear B cell epitopes by applying a threshold score of less than 4.0. These 48 epitopes were then subjected to antigenicity, allergenicity, IFN-γ, and toxicity analysis. Six of these epitopes have antigenic characteristics while also being non-allergenic and non-toxic (Table 1).

Table 1. The physicochemical properties of the six selected B cell epitopes.

Proteins	Epitopes	Antigenicity	IFN-γ	Toxicity
	ASLQRDILTANAKLLD	0.6479	0.12	Non-Toxin
YP_010840880.1	LSKPTMPPVGPVRRLP	0.6088	-0.83	Non-Toxin
	KRPEIRDYTPDFSICQ	0.5532	0.14	Non-Toxin
	LSMIVQTYYPDKFVDF	1.3531	-0.59	Non-Toxin
YP_010840879.1	GGSIEAEILSLRTNQP	0.9792	0.34	Non-Toxin
	CVEQVEQNSENWKQFD	0.7267	0.018	Non-Toxin

3.3 Population Coverage Analysis

In order to determine percentage of the world population would respond to the produced vaccinations, predictions of population coverage based on variants of the HLA interacting to T cell epitopes from the MEV. Countries in Europe (Spain, Germany, France, the United Kingdom, the Netherlands, or Portugal), North America (Mexico, Canada, and the United States), and South America (Brazil, and Peru) all experienced relatively severe YEZV infections through this outbreak, as shown in Figure 2. This suggests the MEV experienced widely used in these regions (Table 2). According to the analysis of population coverage, the YEZV-V2 vaccine candidates proposed to date have the potential to combat Yezo disease worldwide.

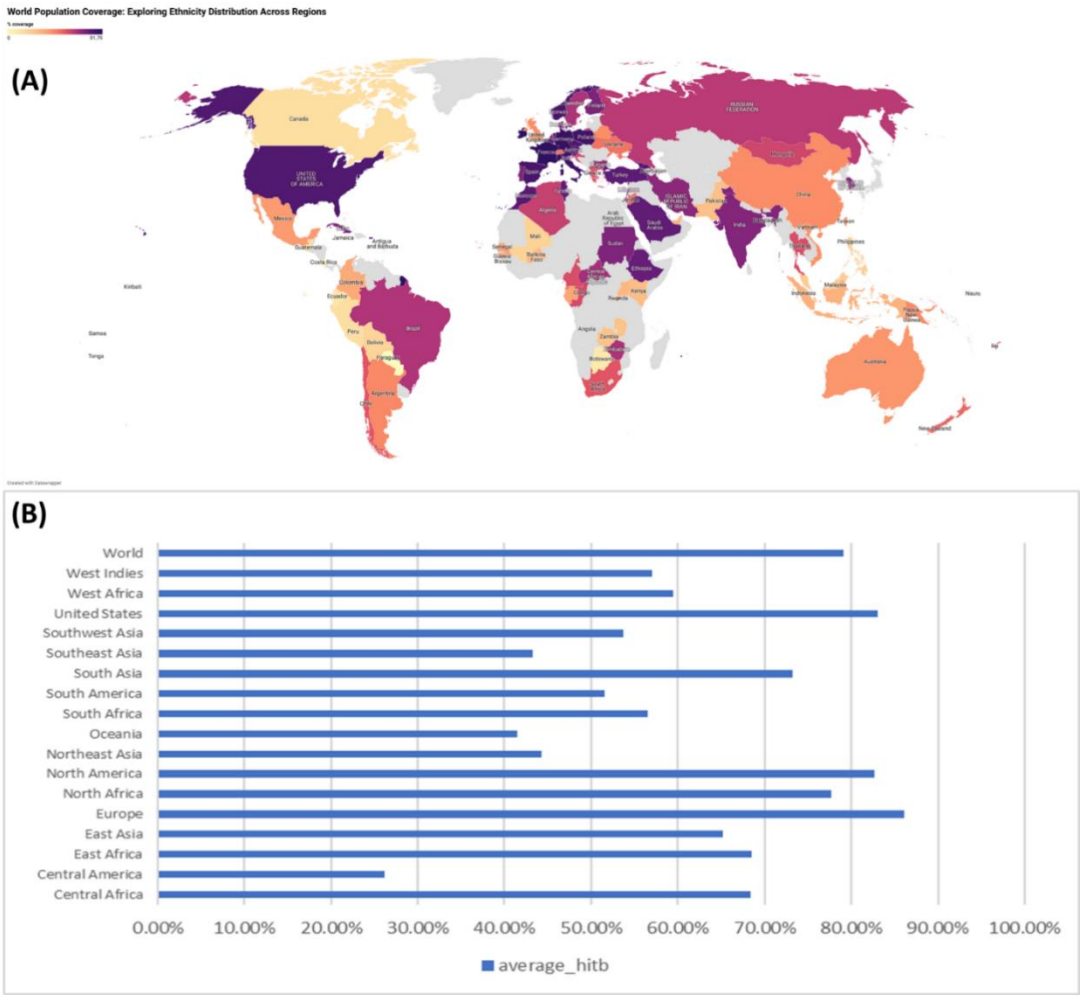

Figure 2. Global population coverage and MHC epitope distribution analysis. (A) Global country-level population coverage. (B) Using the IEDB database to evaluate MHC epitope distribution coverage in highly infected regions of the world.

Table 2. Disparities in multicultural health care coverage.

Region	YP_010840880.1		YP_010840879.1	
	MHC1	MHC2	MHC1	MHC2
East Africa	97.40%	99.18%	97.03%	68.53%
Central America	9.07%	58.10%	8.33%	33.54%
Central Africa	96.31%	98.63%	95.98%	61.73%
North America	99.81%	99.98%	99.67%	83.39%
East Asia	99.40%	99.89%	99.04%	77.97%
North Africa	99.10%	99.79%	98.83%	73.93%
Europe	99.98%	100.00%	99.92%	82.72%
Northeast Asia	97.20%	98.90%	96.81%	58.34%
South Asia	98.00%	99.53%	97.31%	74.71%
South America	96.49%	98.72%	95.99%	47.87%
Oceania	98.58%	99.44%	98.37%	57.94%
South Africa	99.36%	99.56%	99.26%	32.10%
West Africa	98.00%	99.32%	97.39%	63.11%
West Indies	99.34%	99.80%	98.68%	66.69%
Southeast Asia	97.75%	99.07%	97.38%	58.20%
Southwest Asia	97.30%	98.52%	96.18%	42.35%
World	99.76%	99.96%	99.57%	77.74%
Average	93.11	96.96	92.69	62.4

3.4 Chimeric MEV Designingng, Immunological and Physiochemical Properties

A total of six distinct components, including CTL epitopes, HTL epitopes, interpreted epitopes, PADRE sequences, an adjuvant, and a His-tag sequence, were utilized in the designing of the final MEV. The N-terminus adjuvants, namely HBHA, β-defensin, HBHA conserved, and Ribosomal protein, was joined to the first CTL epitope via an EAAAK linker were used in the designing of four different vaccines constructs (Table S2). The EAAAK linker used increase its immunogenicity (Figure 3).

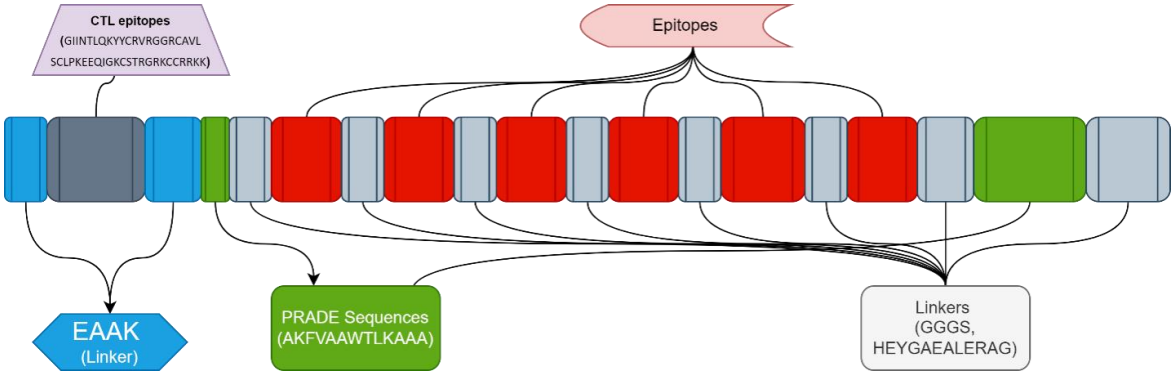

Figure 3. A MEV construct shown schematically.

Assessment of the vaccine's immunogenic and physical-chemical characteristics was done once the structure of the vaccine was designed. The vaccine demonstrated non-allergic and antigenic properties, but had a high antigenic property (0.7831 to 0.4%), according to later immunological tests. The vaccine's molecular weight, theoretical isoelectric points (pI) , GC content and Aliphatic index was in acceptable range (Table 3). Additionally, research revealed an average the half-life of thirty hours for bacteria, a half-life of over twenty hours for yeast investigations, and a half-life of over 10 hours for *E. coli* tests. The GRAVY index, which measures how hydrophilic a substance. As a consequence, the analysis supported the MEV as a possible vaccine candidate. In addition, none of the 4 vaccine constructs (YEZV-V4 being the only exception) triggered any sort of adverse reaction and these vaccine prototypes were predicted as non-toxic and non-allergic.

Table 3. Evaluation of vaccine construct physiochemical.

Vaccine constructs	Amino acid	Molecular weight (Da)	Instability index	Theoretical PI	GRAVY	GC content	CAI	Aliphatic index
YEZV-V1 with HBHA adjuvant	356	38095.25	36.95	4.75	-0.367	75.19	0.96	77.25
YEZV-V2 with β-adjuvant	242	25627.80	33.81	8.39	-0.344	66.28	0.96	62.36
YEZV-V3 with HBHA conserved adjuvant	347	36977.03	41.49	4.69	-0.335	80.06	0.97	77.32
YEZV-V4 with Ribosomal protein adjuvant	326	33836.01	26.94	4.71	-0.093	81.01	0.97	78.10

3.5 2D and 3D Structure Analysis and Validation

The chemical interactions between an immunization and antigen receptor protein must be studied in the context of a stable, functional Two dimensional and three-dimensional structure. 2D structure of vaccine construct was designed for all vaccine constructs using PSIPRED v3.3 Webserver. Prediction of vaccine structures was exposed via the Swiss Models server for homology simulations (Figure S1) and validated through ERRAT by mean of energies. A structural validation investigation was carried out to ensure the dependability of the projected constructions (Figure 4). We discovered that 99.0% of residues in V1 (HBHA adjuvant), 84.5% in V2 (With β-definsin adjuvant), 84.5% in V 3 (HBHA conserved adjuvant), plus 89.4 percent in V4 (50S Ribosomal protein adjuvant) were positioned in the favored region within the plots after creating Ramachandran plots depending on the vaccine design (Figure 4) and (Figure S2-S4). The enhanced vaccine constructions were assessed using the ERRAT approach, Z scores evaluated by the ProSA-web server and the results of an RAMPAGE analysis, using the ERRAT online tool, confirmed the good quality of the vaccine 3D structures (Table 4) [59].

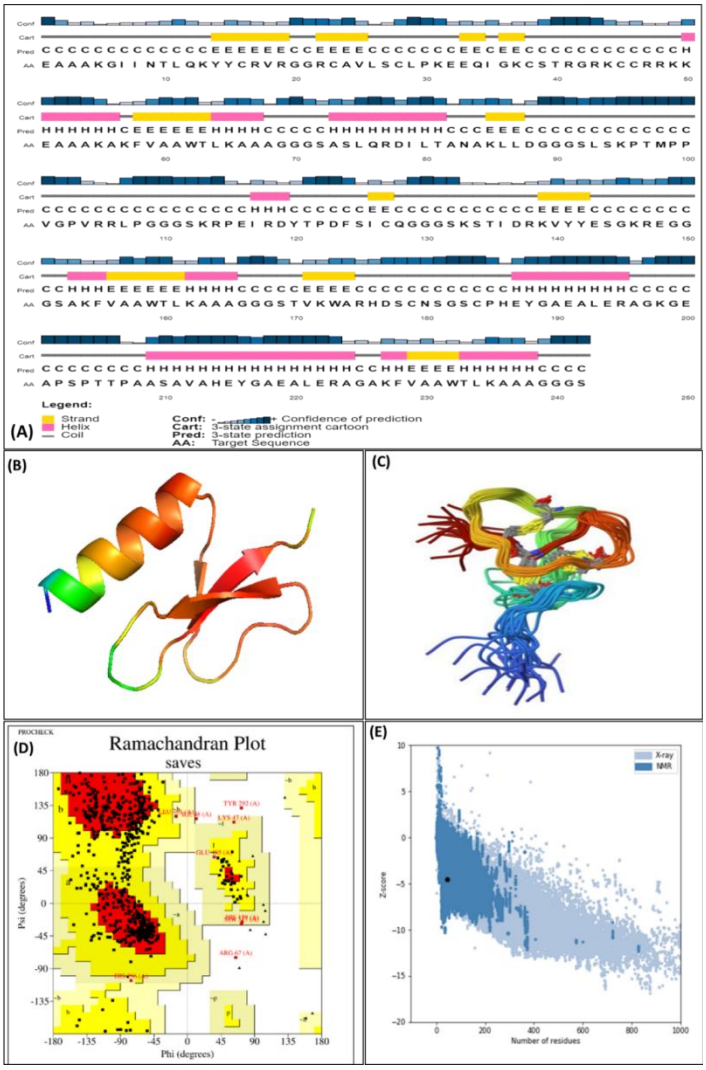

Figure 4. Development and validation of a tertiary structure model for a YEZV-V2 construct. **(**A) 2D structure presentation of vaccine construct. (B) The refined 3D structure from swiss model server. (C) The 3D structure of YEZV is almost similar to this known structure of PDB (ID: 2LXO). (D) Ramachandran plot analysis of the MEV Construct. (E) Evaluation of the refined 3d structure: Z-score analysis using the ProSA-Web Server.

Table 4. Validating vaccine design and 3D structural analysis using PROCHECK, ERRAT (Ramachandran plot favored region), and ProSA-Web Server.

S. no	PROCHECK	ERRAT	ProSA (Z-score)
1	86.9%	90.583	-2.1
2	97.4%	93.75	-4.52
3	89.5%	97.0149	-0.49
4	82.8%	99	-4.11

3.6 MEV Docking with HLA and TLRs Receptors

To evaluate the immunological compatibility of the designed MEV constructs, molecular docking analyses were performed between the MEVs and key immune receptors, including human HLA and TLR3, TLR4, and TLR8. Docking was carried out using the HDock server, followed by refinement of the top-ranked complexes using HawkDock to account for protein flexibility and to obtain more reliable binding energy estimations. Among all constructs, the V2 construct demonstrated the strongest and most consistent binding affinity across HLA and TLR receptors, indicating superior immunological potential. In the HLA-V2 complex, the V2 construct was observed to occupy the canonical peptide-binding groove of the HLA molecule (Figure 5A), suggesting a structurally favorable orientation for antigen processing and presentation to T cells. This interaction supports the ability of the V2 construct to effectively engage adaptive immune mechanisms. For innate immune receptors, docking analyses revealed that the V2 construct interacts predominantly with the extracellular leucine-rich repeat

(LRR) domains of TLR3, TLR4, and TLR8, which are known to be responsible for ligand recognition and initiation of downstream signaling (Figure 5B-D). The localization of the V2 construct within these functionally relevant binding pockets indicates that the interactions are biologically meaningful rather than nonspecific surface contacts, and may contribute to receptor activation and innate immune stimulation. Binding energy analysis further supported these observations. The HLA-V2 complex exhibited a notably strong binding energy of -71.28 kcal/mol, which was substantially lower (more favorable) than those observed for the other constructs. Similarly, V2 showed strong binding affinities with TLR4 (-62.03 kcal/mol), TLR3 (-38.95 kcal/mol), and TLR8 (-27.91 kcal/mol), outperforming the remaining vaccine constructs (Table 5). These results highlight the structural stability and high-affinity interactions of the V2 construct with both adaptive and innate immune receptors. Overall, the preferential binding of the V2 construct within key functional regions of HLA and TLR receptors, combined with its favorable binding energy profile, supports its selection as the most promising MEV candidate for further immunogenic evaluation.

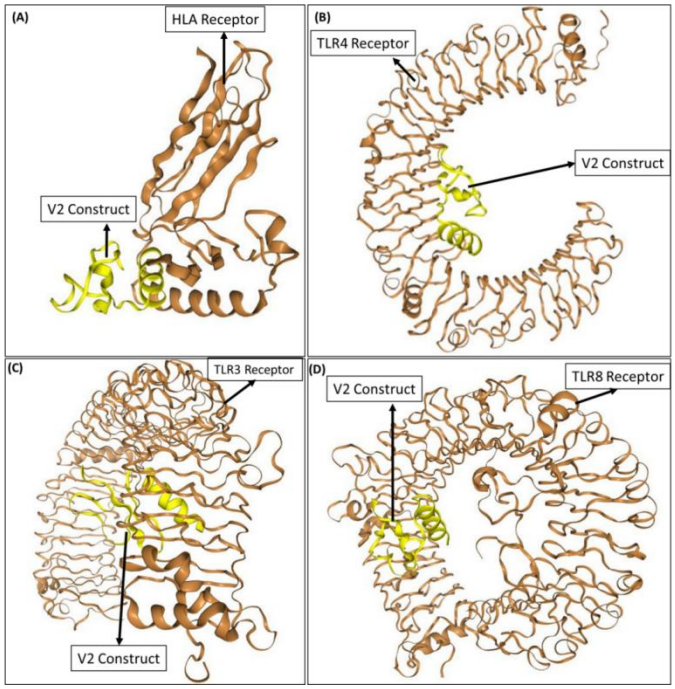

Figure 5. Docking analysis of the YEZV-V2 construct with immune receptors. (A) V2 construct positioned within the peptide-binding groove of the HLA receptor, supporting antigen presentation. (B) Docked complex of TLR4 receptor showing V2 interaction within the extracellular LRR domain. (C) TLR3 receptor-V2 complex highlighting binding near ligand-recognition regions. (D) TLR8 receptor-V2 complex demonstrating stable interaction within the functional ectodomain.

Table 5. Docking results of HLA and TLRs receptor with vaccines constructs.

S. no	Receptor with vaccine construct	Docking Score	Ligand RMSD (A)	Binding energy (kcal/mol)
1	HLA-V1	-262.08	78.87	-13.62
2	HLA-V2	-229.68	61.26	-71.28
3	HLA-V3	-248.64	69.79	-22.81
4	HLA-V4	-226.10	35.04	-21.71
5	TLR4-V1	-312.43	79.83	-4.27
6	TLR4-V2	-266.51	26.91	-62.03
7	TLR4-V3	-370.48	61.14	7.92
8	TLR4-V4	-200.17	55.05	10.5
9	TRL3-V1	-385.59	99.27	2.71
10	TRL3-V2	-278.24	29.76	-38.95
11	TRL3-V3	-277.59	96.78	-3.69
12	TRL3-V4	-272.16	99.39	-1.7
13	TRL8-V1	-368.66	59.98	-13.82
14	TRL8-V2	-274.59	63.99	-27.91
15	TRL8-V3	-301.52	73.95	6.13
16	TRL8-V4	-240.85	73.30	-15.9

3.7 Normal-Mode Analyses

The YEZV-V2 construct demonstrated the lowest global energy after binding on the TLR4 and HLA receptors was chosen as the final version. MD simulations with energy minimization & protein stability analyses were used to evaluate the stability for the YEZV-V2-HLA complex. The iMODS Webserver was used to conduct a simulation analysis of the movement of molecules and atoms inside the intended vaccine in a system that is biological system [43]. Normal modes analysis (NMA) is used by the iMODS Webserver to characterize the coordinated functional mobility of macromolecules. The frequency of a normal mode is proportional to the magnitude of the relative motion produced, and the direction of molecular displacement is represented by the deformation vector. These measures allow for an evaluation of molecular adaptability in a cellular setting. The NMA characterization of the YEZV-V2-HLA docked complex are shown in the Figure 6. Iterative deformation at the lowest modes was applied to the input structure in order to probe attainable transitions, and RMSD was minimized via locally and globally aligning the frameworks. The complex's main-chain deformability is depicted as peaks in the deformability graph (Figure 6A), which indicate regions of proteins flexibility. Main chain residues tend to be higher in flexible regions like hinges and linkers and decrease in stiff regions. The B-factor, which was calculated using NMA, characterizes the magnitude of atomic motions within molecular complex near the equilibrium conformation, Figure 6B shows a link between the PDB scores (indicating the average RMSD) and the mobility of the tethered complex NMA as depicted by the B-factor graph. The stiffness that moves can be calculated by calculating the eigenvalues of the normal modes, which directly represent the amount of energy needed to deform the structure. The lower the eigenvalues, the more easily the alpha carbon atoms can be deformed. Figure 6C shows that the eigenvalue for the YEZV-V2/HLA complex is 1.030787e-05, confirming the stability of the complex. Each of the normal modes of the complex is represented by a different purple and green bar on the variance graph, Figure 6D depicts an inversely-related graph, which sheds light on the system's dynamics. Coupling between pairs of proteins is shown in Figure 6E as red, white, and blue patches representing correlated, uncorrelated, and anti-correlated atomic movements, respectively, inside dynamic sections of the complex molecule. The Ca atomic Cartesian coordinates were used to calculate the correlation matrix according to Equation 2 [60]. The atomic connections are specified by the complex's elastic network model. The graph's dots stand in for the springs that link individual atomic pairs. Dots of different colors signify different levels of spring stiffness, in Figure 6F, darker greys represent stiffer parts while lighter dots represent more flexible regions.

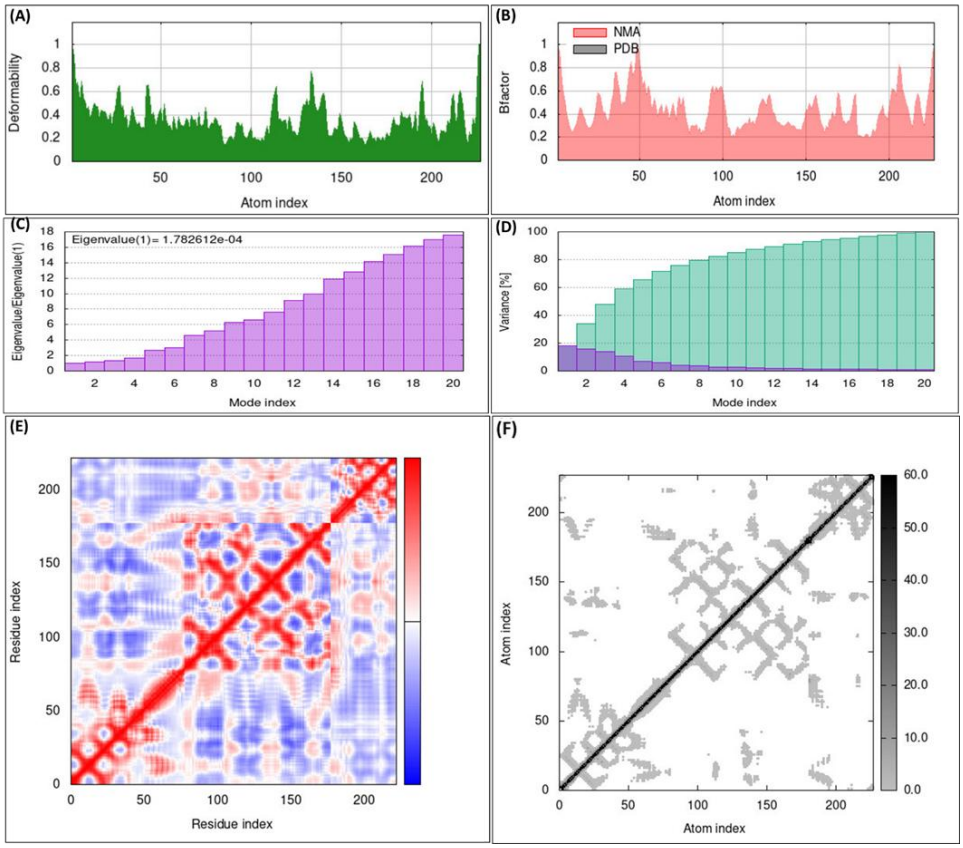

Figure 6. The results of MD simulations of the YEZV-V2 and HLA complexes deploying iMODS server. (A) Deformability. (B) B-factor. (C) eigenvalues. (D) Individual variances are depicted by purple bars, while cumulative variances are shown by green bars. (E) Elastic network model (grey patches) and covariance matrix (blue), uncorrelated (white), nor correlated (red) movement of paired residues. (F) showing the flexible and stiffer areas.

3.8 MD Simulation Analyses

A comparative MD simulation analysis was performed to evaluate the structural stability and dynamic behavior of the YEZV-V2-HLA complex relative to the apo HLA receptor. Root Mean Square Deviation (RMSD) and Root Mean Square Fluctuation (RMSF) analyses were conducted using C-alpha atoms to assess global and residue-level conformational changes throughout the 150 ns simulation. As shown in Figure 7, the apo HLA receptor exhibited higher RMSD fluctuations over the simulation period, reflecting its intrinsic conformational flexibility. In contrast, the YEZV-V2-HLA complex stabilized rapidly within the initial ~10 ns and maintained a consistently lower RMSD profile thereafter, indicating enhanced structural stability upon vaccine binding. A minor RMSD increase observed around 35-40 ns for the complex remained within an acceptable range and likely represents adaptive conformational rearrangement rather than destabilization. Overall, the reduced RMSD values of the ligand-bound system demonstrate sustained occupancy of the YEZV-V2 construct within the HLA binding groove. Residue-wise flexibility analysis (Figure 8) further supported these observations. The YEZV-V2-HLA complex displayed reduced Residue-wise Root Mean Square Fluctuation (RMSF) values across most residues compared with the apo receptor, particularly within the peptide-binding region. Elevated fluctuations were primarily confined to terminal and loop regions, which are inherently flexible and distal from the interaction interface. These results confirm that binding of the YEZV-V2 construct restricts excessive residue mobility and enhances receptor rigidity in functionally important regions [61-63].

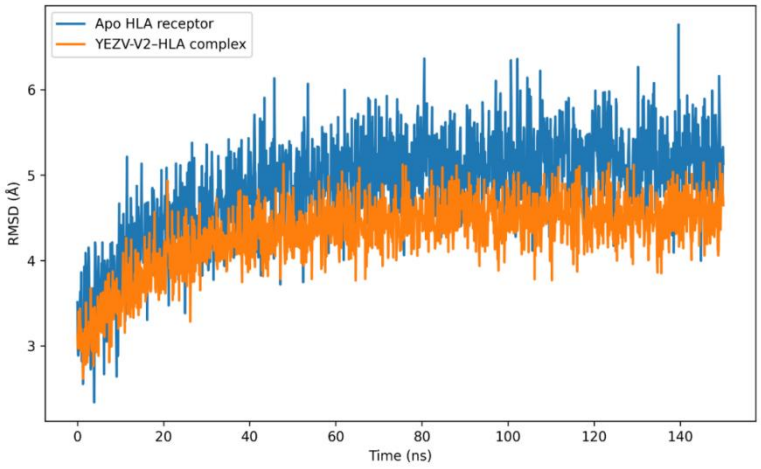

Figure 7. Comparative RMSD analysis of the apo HLA receptor and the YEZV-V2-HLA complex over a 150 ns MD simulation. RMSD values were calculated using C-alpha atoms. The YEZV-V2-HLA complex shows reduced structural deviation and earlier stabilization compared to the apo receptor, indicating enhanced conformational stability upon vaccine binding.

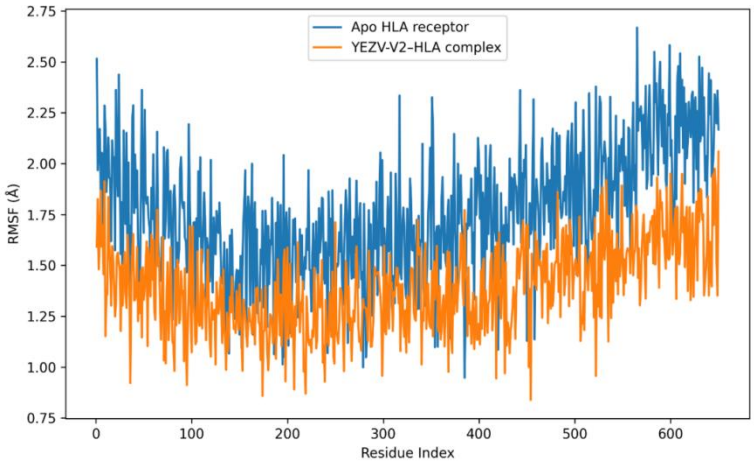

Figure 8. RMSF comparison between the apo HLA receptor and the YEZV-V2-HLA complex calculated using C-alpha atoms. The YEZV-V2-HLA complex exhibits reduced residue-level flexibility across most regions, particularly within the peptide-binding domain, indicating stabilization of the receptor upon vaccine binding.

Secondary structure evolution was monitored throughout the 150 ns MD simulation and is illustrated in Figure 9. The analysis shows that the overall secondary structural content of the HLA receptor remains stable over time, with no evidence

of large-scale unfolding or abrupt structural transitions in either the apo or ligand-bound states. The percentage of secondary structure elements (%SSE) fluctuated within a narrow range throughout the simulation, indicating preservation of the global fold.

The residue-wise secondary structure representation further highlights differences between the two systems. In the apo HLA receptor (Figure 9A), secondary structure elements exhibit greater residue-level variability, with an increased presence of coil regions, particularly within loop and terminal segments. In contrast, the YEZV-V2-HLA complex (Figure 9B) shows enhanced persistence of α-helical and β-sheet regions, represented by continuous red horizontal lines across extended simulation periods. These structured regions are largely maintained in the ligand-bound complex, while flexible coil regions (blue lines) remain confined mainly to peripheral and linker regions.

The improved preservation of α-helices and β-sheets in the YEZV-V2-HLA complex correlates well with the reduced RMSD and RMSF values observed for the ligand-bound system. As reported previously, rigid secondary structure elements such as helices and sheets contribute to overall conformational stability, whereas flexible coils and loops account for localized fluctuations. Collectively, these findings indicate that binding of the YEZV-V2 construct promotes secondary structure stability of the HLA receptor during the simulation.

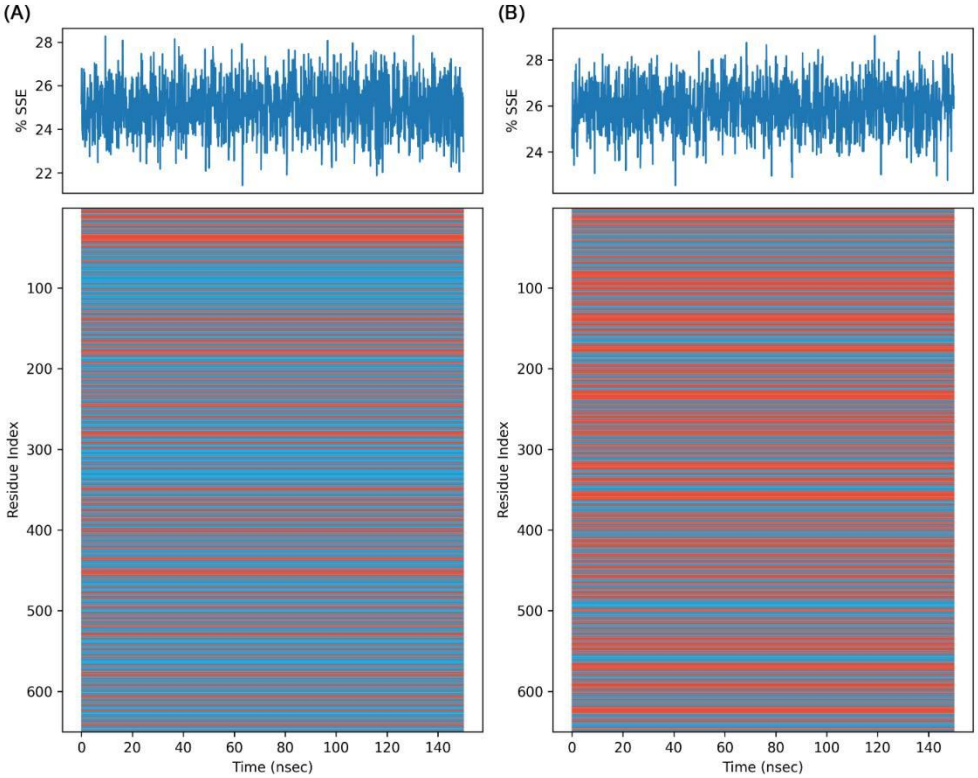

Figure 9. Secondary structure evolution during the 150 ns MD simulation shown in a DSSP-like continuous line representation. (A) APO HLA receptor and (B) iso-HB2 HLA receptor. The upper panels display the percentage of secondary structure elements (%SSE) over time, while the lower panels show residue-wise secondary structure distribution as continuous horizontal lines, where red lines represent α-helices and β-sheets and blue lines indicate coil regions. The comparison highlights residue-level structural variation between the two systems.

3.9 Immune Simulation of MEV

The C-ImmSim 10.1 web server was used to computationally predict host immune system responses to the YEZV-V2 vaccine construct. The simulation was designed to model the temporal dynamics of antigen clearance and adaptive immune activation based on established immunological algorithms. The predicted antibody kinetics indicated an initial IgM-dominated primary response followed by substantial increases in IgG1 and IgG2 titers during secondary and tertiary exposures, corresponding to simulated memory formation and isotype switching (Figure 10A-D). Concurrently, simulated antigen levels decreased following repeated exposures, consistent with modeled antigen neutralization.

The simulation also predicted enhanced B cell proliferation, activation of $CD4^+$ helper and $CD8^+$ cytotoxic T lymphocytes, and increased dendritic and macrophage activity following vaccine exposure (Figure 10E-H). Cytokine secretion dynamics suggested elevated IL-2, IFN-γ, and IL-12 concentrations, which are typically associated with Th1-biased immune

responses (Figure 10I). It is important to note, however, that these results represent *computational predictions* generated under predefined parameters and do not constitute experimental evidence of immune protection or long-term immunological memory. While the modeled profiles provide valuable insight into the theoretical immunogenic potential of the YEZV-V2 construct, *in vitro* and *in vivo* validation will be essential to confirm these predicted trends in biological systems.

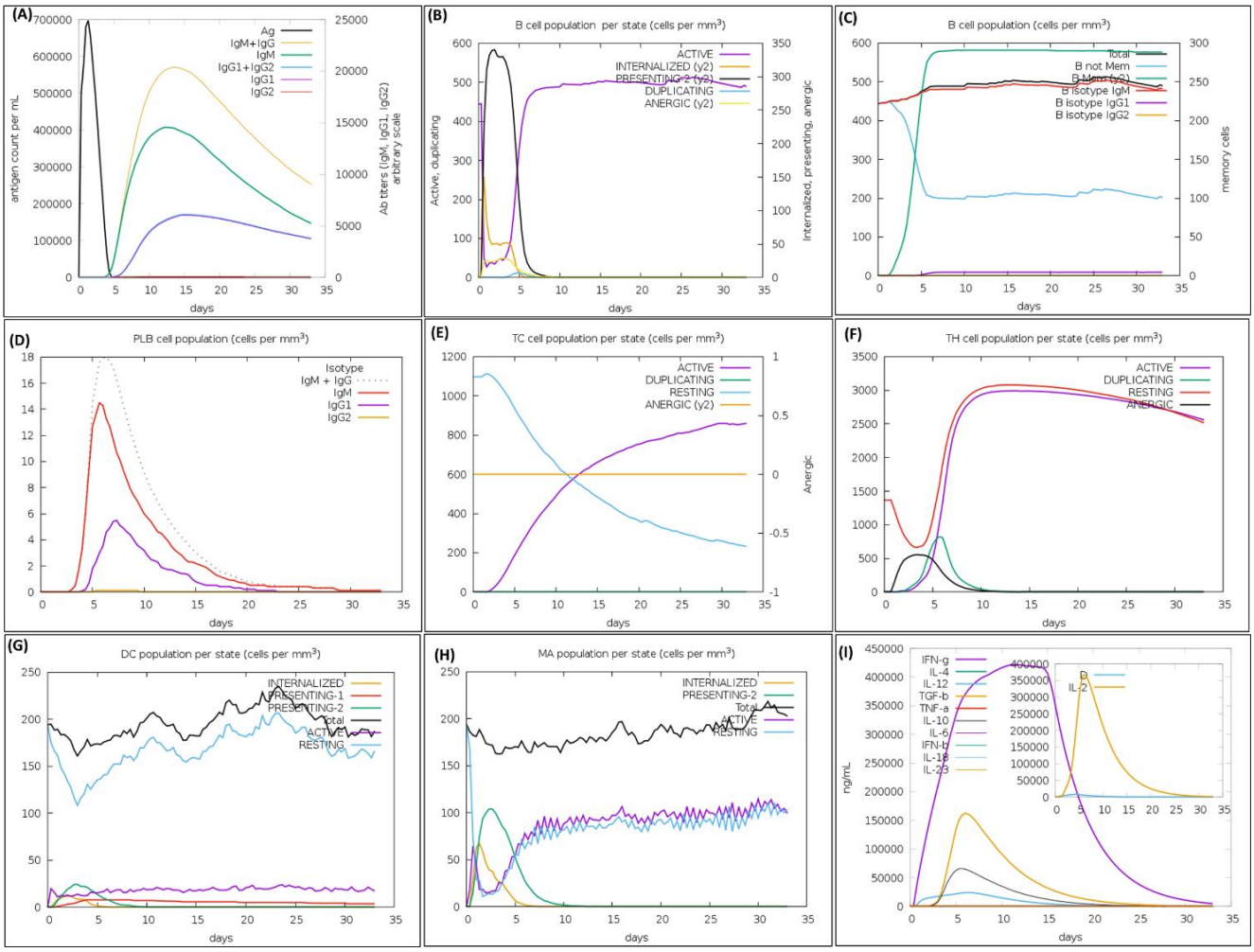

Figure 10. The Influence of Vaccine Injections upon Serum Antibody and Plasma Antigen Levels: An *in vivo* Study. (B) How Vaccinations Affect B cell Counts and Antigen Concentrations. Improved B cell response and lower antigen levels after vaccine (C). Number of plasma B lymphocytes broken down by isotype (IgM, IgG1, and IgG2) is shown in (D). Increased numbers of both types of T cells (T cytotoxic and T helper) after repeated antigen exposure (E, F). Dendritic cells, macrophages, or killer cells in the body (NK) are increased in number after receiving a (G-H) vaccine. (I) The inset plot shows increased IL-2 neutrophil growth factor levels along with other cytokines and interleukins after repeated antigen exposure.

3.10 *E. coli* cloning and Codon Optimization

The capability of the vaccine structure to be expressed is the primary aspects in vaccine design. The focused was on the *E. coli* K12 races because of their distinct expression mechanism that requires codon modification in order to properly express the constructed gene. The JCAT server used to verify the codon optimization inside the *E. coli* transcription system. The codon adapting index (CAI) for the best cDNA was 1.0, and that its GC content was 49.77%. These results show that the vaccine design has a good chance of being expressed in an *E. Coli* K-12 strain. A recursive plasmid sequence was created with the help of the SnapGene program. The plasmid vector pET28a (+) was modified by inserting the modified codon sequences of the final vaccine construct, referred to as V2. This systematic approach enabled that heterologous cloning plus subsequent expression inside the *E. coli* system could be successfully integrated (Figure 11).

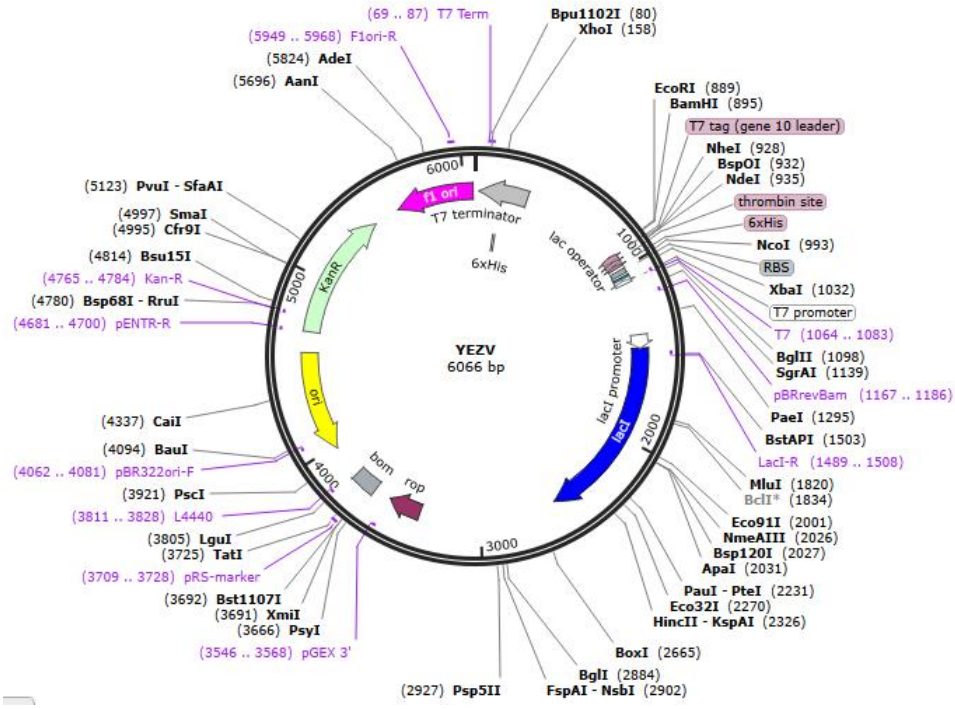

Figure 11. *In-silico* cloning of YEZV gene in pET28a (+) (a restriction cloning vector) in *E. coli* host.

3.11 Secondary Structure of Vaccine mRNA

The mRNA vaccine precursor's final circle, extending from the 50 to 30 terminal, was intricately designed featuring 50 homology arms, T1, CBV3 IRES, a designed sequence of spacers, Kozak-tPA, EAAAK linker, and an innovative combination of adjuvants and epitopes. The meticulously constructed sequence concludes with 30 homology arms, forming a comprehensive and promising design for an mRNA vaccine. This visually engaging representation underscores the precision and creativity employed in developing an advanced vaccine precursor (Figure 12A).

Furthermore, the mRNA's structural integrity was evaluated through the RNAfold server, revealing a MFE secondary structure at -434.70 kcal/mol and a Centroid secondary structure at -389.20 kcal/mol. These findings underscore the stability of the mRNA, instilling confidence in its resilience post-production (Figure 12B-C).

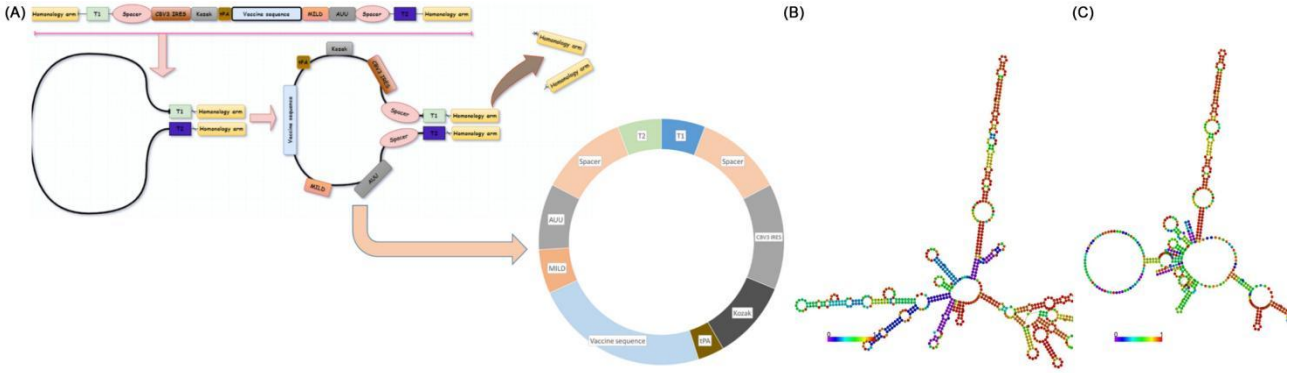

Figure 12. Construction of circRNA vaccine (A) structure of DNA and liner RNA and circulation of RNA vaccine and their circular RNA vaccine structure (B-C) secondary structure of circular RNA vaccine.

4. Discussion

The exponential increase in YEZV infections poses a potential public health concern, even though currently reported human cases remain geographically restricted to East Asia. At present, no licensed vaccine or targeted therapeutic intervention exists for YEZV [64,65]. To address this gap, we employed a structure-based immunoinformatics approach to design a multi-epitope, circRNA vaccine construct, aimed at inducing both humoral and cellular immune protection. This strategy

was built upon the identification of highly antigenic, non-allergenic epitopes predicted to elicit T cell and B cell-mediated responses against YEZV, leveraging its proteomic information and known orthonairovirus immunogenic domains.

The integration of both B cell and T cell epitopes is essential for balanced immune activation. Major histocompatibility complex (MHC) class I and class II epitopes mediate antigen presentation to cytotoxic and helper T cells, respectively, thus triggering a coordinated adaptive immune response [66]. Our designed construct incorporated six highly antigenic epitopes linked via EAAAK and GGGS linkers and adjuvanted with β-defensin to enhance immunogenicity and stability. The physicochemical analysis confirmed high thermostability (positive aliphatic index) and favorable hydropathic properties (negative GRAVY value), indicating its potential for expression and folding efficiency [67,68]. These findings are consistent with previous vaccine modeling studies for *Crimean-Congo hemorrhagic fever virus* (CCHFV) and *Nairobi sheep disease virus*, which also emphasized the importance of hydrophobic stabilization and adjuvant optimization to achieve robust antigenicity [69,70].

Structurally, our 3D-modeled vaccine displayed a reliable conformation with a ProSA Z-score of -4.52 and PROCHECK validation within acceptable Ramachandran limits, confirming the model's quality. The strong binding affinities observed between the YEZV-V2 construct and host immune receptors (HLA and TLRs) suggest its potential to induce both innate and adaptive immune pathways. Comparable binding patterns have been reported for other Orthonairovirus MEVs, such as those targeting the CCHFV GP38 protein, where similar HLA affinities correlated with improved immune activation. The HawkDock and HDOCK docking scores (up to -71.28 kcal/mol) support these interactions, aligning with docking data from *in silico* Ebola and SARS-CoV-2 vaccine studies [71-73]. NMA revealed a low eigenvalue (1.782612e-04), indicating high structural flexibility and molecular stability, essential for receptor compatibility. This dynamic stability is further corroborated by MD simulation analyses, showing minimal RMSD fluctuations and stable RMSF profiles throughout the 150 ns simulation period. These patterns mirror observations in recent computational vaccine designs against tick-borne encephalitis and Zika viruses, where stability of receptor-ligand interactions predicted improved immunogenic performance in wet-lab validations [74]. The immune simulation outcomes predicted a strong secondary and tertiary immune response, dominated by elevated IgM and IgG titers, as well as the expansion of memory B and T cells. While these findings are promising, we emphasize that *in silico* immune simulations, such as those performed via C-ImmSim, are predictive and not definitive. Their results should be interpreted as indicative trends that require empirical confirmation through *in vitro* and *in vivo* studies. Nonetheless, the simulated cytokine patterns (notably IL-2 and IFN-γ) suggest a Th1-biased response, which is desirable for antiviral defense. Compared with traditional peptide vaccines, the proposed circRNA-based mRNA vaccine platform offers distinct theoretical advantages. Circular RNA molecules exhibit increased structural stability, extended translational persistence, and reduced innate immune sensing compared to linear mRNAs, making them attractive for durable immune activation. Recent studies by Wesselhoeft et al. (2023) and Liu et al. (2024) demonstrated that circRNA vaccines can maintain antigen expression up to 48 hours longer than conventional mRNA constructs, leading to enhanced neutralizing antibody titers [18,75]. Our design integrates the CBV3 IRES and group I catalytic introns to promote efficient circularization and cap-independent translation-features not explored in prior YEZV-related studies. This represents a novel contribution of our work to the Orthonairovirus vaccine field. In summary, this study introduces a computationally optimized, structurally validated, and immunologically potent circRNA-based MEV candidate against YEZV. The combined docking, simulation, and immune profiling analyses provide a strong theoretical basis for future experimental validation. However, we acknowledge the need for laboratory confirmation of predicted immunogenicity and stability, as computational predictions alone cannot fully replicate biological complexity. Ultimately, the integration of immunoinformatics-driven epitope mapping with circRNA engineering establishes a promising framework for developing next-generation antiviral vaccines, not only against YEZV but also other emerging tick-borne pathogens within the Orthonairovirus genus.

Limitations and future perspectives: While this study provides a comprehensive computational framework for the design and evaluation of a circRNA-based MEV against YEZV, it remains entirely predictive in nature and requires experimental confirmation. All immunogenicity, stability, and molecular interaction results were derived from *in silico* analyses using docking, MD simulations, and immune response modeling tools. These computational predictions, while robust, cannot fully replicate the complex biological and immunological processes occurring *in vivo*. Future work should therefore prioritize experimental validation through *in vitro* assays such as antigen expression analysis, epitope binding affinity measurement (via ELISA or flow cytometry), and cytokine release profiling in mammalian cell models. Furthermore, *in vivo* validation in animal models will be essential to confirm the immunogenicity, protective efficacy, and safety of the proposed construct. In addition, comparative studies should be undertaken to evaluate the translational advantages of the circRNA vaccine platform over conventional linear mRNA vaccines, particularly regarding stability, half-life, and immune activation efficiency. The incorporation of delivery systems such as lipid nanoparticles (LNPs) or extracellular vesicles may further enhance the vaccine's delivery and performance. Finally, continuous genomic surveillance of YEZV and related orthonairoviruses will be vital for updating epitope databases and ensuring that the proposed vaccine construct remains effective against newly emerging strains. Overall, this work lays a strong foundation for the experimental translation of computational vaccine design into practical, next-generation RNA immunization strategies.

5. Conclusion

Immunoinformatics approaches used for constructing a multi-epitope mRNA vaccine against YEZV by focusing on its conserved proteins. The YEZV-V2 vaccines was found to have suitable sensitivity to interacting through the HLA receptor of the human system of immunity, as well as high primary and secondary immunological responses. This communication is crucial for the development of adaptive immunity and the efficient suppression of infections. Strong and stable adherence of MEV-V2 to receptors (TLRs and HLA) was further validated by the MD Simulation, providing further evidence for the importance of these chemical interactions. According to immunological and physiochemical testing, YEZV-V2 is the best vaccine construct because it has the lowest binding energy towards HLA and TLRs receptors.

Conflict of Interest

The authors declare no conflict of interest.

Generative AI Statement

The authors declare that no Gen AI was used in the creation of this manuscript.

References

[1] Kodama F, Yamaguchi H, Park E, Tatemoto K, Sashika M, Nakao R, et al. A novel nairovirus associated with acute febrile illness in Hokkaido, Japan. Nature Communications, 2021, 12(1), 5539. DOI: 10.1038/s41467-021-25857-0
[2] Ji X, Guo C, Dai Y, Chen L, Chen Y, Wang S, et al. Genomic characterization and molecular evolution of sapovirus in children under 5 years of age. Viruses, 2024, 16(1), 146. DOI: 10.3390/v16010146
[3] Matsuno K. Yezo virus and emerging orthonairovirus diseases. Uirusu, 2021, 71(2), 117-124. DOI: 10.2222/jsv.71.117
[4] Lv X, Liu Z, Li L, Xu W, Yuan Y, Liang X, et al. Yezo virus infection in tick-bitten patient and ticks, Northeastern China. Emerging Infectious Diseases, 2023, 29(4), 797-800. DOI: 10.3201/eid2904.220885
[5] Kartashov M, Svirin K, Zheleznova A, Yanshin A, Radchenko N, Kurushina V, et al. First report of the Yezo virus isolates detection in Russia. Viruses, 2025, 17(8), 1125. DOI: 10.3390/v1708112
[6] Chen ZY, Zhang J, He PJ, Xiong T, Zhu DY, Zhu WJ, et al. Characteristics of viral ovarian tumor domain protease from two emerging orthonairoviruses and identification of Yezo virus human infections in Northeastern China as early as 2012. Journal of Virology, 2025, 99(2), e0172724. DOI: 10.1128/jvi.01727-24
[7] Ho PL, Miyaji EN, Oliveira ML, Dias Wde O, Kubrusly FS, Tanizaki MM, et al. Economical value of vaccines for the developing countries-the case of Instituto Butantan, a public institution in Brazil. PLOS Neglected Tropical Diseases, 2011, 5(11), e1300. DOI: 10.1371/journal.pntd.0001300
[8] Ariizumi T. Studies on the pathogenicity of emerging orthonairovirus, Yezo virus, and effects of antiviral agents against Yezo virus using a mouse model. Sapporo, Hokkaido University, 2025.
[9] Zhang MZ, Bian C, Ye RZ, Cui XM, Yao NN, Yang JH, et al. A series of patients infected with the emerging tick-borne Yezo virus in China: an active surveillance and genomic analysis. The Lancet Infectious Diseases, 2025, 25(4), 390-398. DOI: 10.1016/S1473-3099(24)00616-9
[10] Ali SL, Ali A, Alamri A, Baiduissenova A, Dusmagambetov M, Abduldayeva A. Genomic annotation for vaccine target identification and immunoinformatics-guided multi-epitope-based vaccine design against Songling virus through screening its whole genome encoded proteins. Frontiers in Immunology, 2023, 14, 1284366. DOI: 10.3389/fimmu.2023.1284366
[11] Bidmos FA, Siris S, Gladstone CA, Langford PR. Bacterial vaccine antigen discovery in the reverse vaccinology 2.0 Era: Progress and challenges. Frontiers in Immunology, 2018, 9, 2315. DOI: 10.3389/fimmu.2018.02315
[12] Zhang L. Multi-epitope vaccines: A promising strategy against tumors and viral infections. Cellular & Molecular Immunology, 2018, 15(2), 182-184. DOI: 10.1038/cmi.2017.92
[13] Nosrati M, Behbahani M, Mohabatkar H. Towards the first multi-epitope recombinant vaccine against Crimean-Congo hemorrhagic fever virus: A computer-aided vaccine design approach. Journal of Biomedical Informatics, 2019, 93, 103160. DOI: 10.1016/j.jbi.2019.103160
[14] Apanasevich M, Dubovitskiy N, Derko A, Khozyainova A, Tarasov A, Kokhanenko A, et al. Genomic characterization of a novel Yezo virus revealed in *Ixodes pavlovskyi* tick virome in Western Siberia. Viruses, 2025, 17(10), 1362. DOI: 10.3390/v17101362
[15] Hajighahramani N, Nezafat N, Eslami M, Negahdaripour M, Rahmatabadi SS, Ghasemi Y. Immunoinformatics analysis and *in silico* designing of a novel multi-epitope peptide vaccine against Staphylococcus aureus. Infection, Genetics and Evolution, 2017, 48, 83-94. DOI: 10.1016/j.meegid.2016.12.010
[16] Sette A, Livingston B, McKinney D, Appella E, Fikes J, Sidney J, et al. The development of multi-epitope vaccines: epitope identification, vaccine design and clinical evaluation. Biologicals, 2001, 29(3-4), 271-276. DOI: 10.1006/biol.2001.0297
[17] Starke S, Jost I, Rossbach O, Schneider T, Schreiner S, Hung LH, et al. Exon circularization requires canonical splice signals. Cell Reports, 2015, 10(1), 103-111. DOI: 10.1016/j.celrep.2014.12.002
[18] Wesselhoeft RA, Kowalski PS, Anderson DG. Engineering circular RNA for potent and stable translation in eukaryotic cells. Nature Communications, 2018, 9(1):2629. DOI: 10.1038/s41467-018-05096-6
[19] Qu L, Yi Z, Shen Y, Lin L, Chen F, Xu Y, et al. Circular RNA vaccines against SARS-CoV-2 and emerging variants. Cell, 2022, 185(10), 1728-1744. e16. DOI: 10.1016/j.cell.2022.03.044

[20] Wheeler DL, Barrett T, Benson DA, Bryant SH, Canese K, Chetvernin V, et al. Database resources of the National Center for Biotechnology Information. Nucleic Acids Research, 2007, 35(Database issue), D5-D12. DOI: 10.1093/nar/gkl1031
[21] Doytchinova IA, Flower DR. VaxiJen: A server for prediction of protective antigens, tumour antigens and subunit vaccines. BMC Bioinformatics, 2007, 8, 4. DOI: 10.1186/1471-2105-8-4
[22] Dimitrov I, Flower DR, Doytchinova I. AllerTOP-A server for *in silico* prediction of allergens. BMC Bioinformatics, 2013, 14(Suppl 6), S4. DOI: 10.1186/1471-2105-14-S6-S4
[23] Gasteiger E, Hoogland C, Gattiker A, Duvaud SE, Wilkins MR, Appel RD, et al. Protein identification and analysis tools on the ExPASy server. In: The proteomics protocols handbook, Totowa, NJ: Humana Press, 2005, 571-607. DOI: 10.1385/1-59259-890-0:571
[24] Fleri W, Paul S, Dhanda SK, Mahajan S, Xu X, Peters B, et al. The immune epitope database and analysis resource in epitope discovery and synthetic vaccine design. Frontiers in Immunology, 2017, 8, 278. DOI: 10.3389/fimmu.2017.00278
[25] Kumar J, Qureshi R, Sagurthi SR, Qureshi IA. Designing of nucleocapsid protein based novel multi-epitope vaccine against SARS-COV-2 using immunoinformatics approach. International Journal of Peptide Research and Therapeutics, 2021, 27(2), 941-956. DOI: 10.1007/s10989-020-10140-5
[26] Malik AA, Ojha SC, Schaduangrat N, Nantasenamat C. ABCpred: a webserver for the discovery of acetyl-and butyryl-cholinesterase inhibitors. Molecular Diversity, 2022, 26(1), 467-487. DOI: 10.1007/s11030-021-10292-6
[27] Bui HH, Sidney J, Dinh K, Southwood S, Newman MJ, Sette A. Predicting population coverage of T cell epitope-based diagnostics and vaccines. BMC Bioinformatics, 2006, 7, 153. DOI: 10.1186/1471-2105-7-153
[28] Khan M, Khan S, Ali A, Akbar H, Sayaf AM, Khan A, et al. Immunoinformatics approaches to explore Helicobacter Pylori proteome (Virulence Factors) to design B and T cell multi-epitope subunit vaccine. Scientific Reports, 2019, 9(1), 13321. DOI: 10.1038/s41598-019-49354-z
[29] Dhople V, Krukemeyer A, Ramamoorthy A. The human beta-defensin-3, an antibacterial peptide with multiple biological functions. Biochimica et Biophysica Acta (BBA)-Biomembranes, 2006, 1758(9), 1499-1512. DOI: 10.1016/j.bbamem.2006.07.007
[30] Furci L, Sironi F, Tolazzi M, Vassena L, Lusso P. Alpha-defensins block the early steps of HIV-1 infection: interference with the binding of gp120 to CD4. Blood, 2007, 109(7), 2928-2935. DOI: 10.1182/blood-2006-05-024489
[31] Shiraliyev R, Orman MA. Metabolic disruption impairs ribosomal protein levels, resulting in enhanced aminoglycoside tolerance. elife, 2024, 13, RP94903. DOI: 10.7554/eLife.94903
[32] McGuffin LJ, Bryson K, Jones DT. The PSIPRED protein structure prediction server. Bioinformatics, 2000, 16(4), 404-405. DOI: 10.1093/bioinformatics/16.4.404
[33] Biasini M, Bienert S, Waterhouse A, Arnold K, Studer G, Schmidt T, et al. SWISS-MODEL: modelling protein tertiary and quaternary structure using evolutionary information. Nucleic Acids Research, 2014, 42(W1), W252-W258. DOI: 10.1093/nar/gku340
[34] Shuvo MH, Gulfam M, Bhattacharya D. DeepRefiner: High-accuracy protein structure refinement by deep network calibration. Nucleic Acids Research, 2021, 49(W1), W147-W152. DOI: 10.1093/nar/gkab361
[35] Laskowski RA, MacArthur MW, Moss DS, Thornton JM. PROCHECK: A program to check the stereochemical quality of protein structures. Journal of Applied Crystallography, 1993, 26, 283-291. DOI: 10.1107/S0021889892009944
[36] Vora J, Patel S, Sinha S, Sharma S, Srivastava A, Chhabria M, et al. Molecular docking, QSAR and ADMET based mining of natural compounds against prime targets of HIV. Journal of Biomolecular Structure and Dynamics, 2019, 37(1), 131-146. DOI: 10.1080/07391102.2017.1420489
[37] Wiederstein M, Sippl MJ. ProSA-web: Interactive web service for the recognition of errors in three-dimensional structures of proteins. Nucleic Acids Research, 2007, 35(suppl_2), W407-W410. DOI: 10.1093/nar/gkm290
[38] Artimo P, Jonnalagedda M, Arnold K, Baratin D, Csardi G, de Castro E, et al. ExPASy: SIB bioinformatics resource portal. Nucleic Acids Research, 2012, 40(W1), W597-603. DOI: 10.1093/nar/gks400
[39] Nawab A, An L, Wu J, Li G, Liu W, Zhao Y, et al. Chicken toll-like receptors and their significance in immune response and disease resistance. International Reviews of Immunology, 2019, 38(6), 284-306. DOI: 10.1080/08830185.2019.1659258
[40] Saleem Naz Babari I, Islam M, Saeed H, Nadeem H, Imtiaz F, Ali A, et al. Design, synthesis, *in-vitro* biological profiling and molecular docking of some novel oxazolones and imidazolones exhibiting good inhibitory potential against acetylcholine esterase. Journal of Biomolecular Structure and Dynamics, 2025, 43(10), 5035-5052. DOI: 10.1080/07391102.2024.2306496
[41] Weng G, Wang E, Wang Z, Liu H, Zhu F, Li D, et al. HawkDock: A web server to predict and analyze the protein-protein complex based on computational docking and MM/GBSA. Nucleic Acids Research, 2019, 47(W1), W322-W330. DOI: 10.1093/nar/gkz397
[42] Yan Y, Zhang D, Zhou P, Li B, Huang SY. HDOCK: A web server for protein-protein and protein-DNA/RNA docking based on a hybrid strategy. Nucleic Acids Research, 2017, 45(W1), W365-W373. DOI: 10.1093/nar/gkx407
[43] López-Blanco JR, Aliaga JI, Quintana-Ortí ES, Chacón P. iMODS: Internal coordinates normal mode analysis server. Nucleic Acids Research, 2014, 42(W1), W271-W276. DOI: 10.1093/nar/gku339
[44] Kumar S, Singh A, Kumar B. Identification and characterization of phenolics and terpenoids from ethanolic extracts of Phyllanthus species by HPLC-ESI-QTOF-MS/MS. Journal of Pharmaceutical Analysis, 2017, 7(4), 214-222. DOI: 10.1016/j.jpha.2017.01.005
[45] Ferreira LG, Dos Santos RN, Oliva G, Andricopulo AD. Molecular docking and structure-based drug design strategies. Molecules, 2015, 20(7), 13384-13421. DOI: 10.3390/molecules200713384
[46] Hildebrand PW, Rose AS, Tiemann JKS. Bringing molecular dynamics simulation data into view. Trends in Biochemical Sciences, 2019, 44(11), 902-913. DOI: 10.1016/j.tibs.2019.06.004
[47] Rasheed MA, Iqbal MN, Saddick S, Ali I, Khan FS, Kanwal S, et al. Identification of lead compounds against Scm (fms10) in Enterococcus faecium using computer aided drug designing. Life, 2021, 11(2), 77. DOI: 10.3390/life11020077
[48] Sargsyan K, Grauffel C, Lim C. How molecular size impacts RMSD applications in molecular dynamics simulations. Journal of Chemical Theory and Computation, 2017, 13(4), 1518-1524. DOI: 10.1021/acs.jctc.7b00028
[49] Bhardwaj P, Biswas GP, Mahata N, Ghanta S, Bhunia B. Exploration of binding mechanism of triclosan towards cancer markers

using molecular docking and molecular dynamics. Chemosphere, 2022, 293, 133550. DOI: 10.1016/j.chemosphere.2022.133550
[50] Ali M, Pandey RK, Khatoon N, Narula A, Mishra A, Prajapati VK. Exploring dengue genome to construct a multi-epitope based subunit vaccine by utilizing immunoinformatics approach to battle against dengue infection. Scientific Reports, 2017, 7(1), 9232. DOI: 10.1038/s41598-017-09199-w
[51] Grote A, Hiller K, Scheer M, Münch R, Nörtemann B, Hempel DC, et al. JCat: A novel tool to adapt codon usage of a target gene to its potential expression host. Nucleic Acids Research, 2005, 33(suppl_2), W526-W531. DOI: 10.1093/nar/gki376
[52] Solanki V, Tiwari V. Subtractive proteomics to identify novel drug targets and reverse vaccinology for the development of chimeric vaccine against Acinetobacter baumannii. Scientific Reports, 2018, 8(1), 9044. DOI: 10.1038/s41598-018-26689-7
[53] Kozakov D, Hall DR, Xia B, Porter KA, Padhorny D, Yueh C, et al. The ClusPro web server for protein-protein docking. Nature Protocols, 2017, 12(2), 255-278. DOI: 10.1038/nprot.2016.169
[54] Ali A, Luqman Ali S. A stable mRNA-based novel multi-epitope vaccine designs against infectious heartland virus by integrated immunoinformatics and reverse vaccinology approaches. Viral Immunology, 2025, 38(3), 73-87. DOI: 10.1089/vim.2025.0004
[55] Ali SL, Ali A, Khan A. Identification and assessment of ferroptosis-related genes and their implication as therapeutic agents for pancreatic ductal adenocarcinoma. Annals of Pancreatic Cancer, 2025, 8, 6. DOI: 10.21037/apc-25-2
[56] Gruber AR, Lorenz R, Bernhart SH, Neuböck R, Hofacker IL. The vienna RNA websuite. Nucleic Acids Research, 2008, 36(suppl_2), W70-W74. DOI: 10.1093/nar/gkn188
[57] Ali A. Development of mRNA cancer vaccines: Delivery strategies and immunogenicity optimization. Current Medical Science, 2025, 45(6), 1275-1287. DOI: 10.1007/s11596-025-00127-y
[58] Ali A, Alamri A, Mishra VK, Utegenova A, Askarova G, Baiduissenova A, et al. TZ1391: A computationally designed circular mRNA multi-epitope vaccine candidate against Mycobacterium tuberculosis via TLR3 immunomodulation. BMC Immunology, 2026, 27(1), 23. DOI: 10.1186/s12865-025-00795-4
[59] Mehmood A, Kaushik AC, Wei D. Prediction and validation of potent peptides against herpes simplex virus type 1 via immunoinformatic and systems biology approach. Chemical Biology & Drug Design, 2019, 94(5), 1868-1883. DOI: 10.1111/cbdd.13602
[60] Ichiye T, Karplus M. Collective motions in proteins: a covariance analysis of atomic fluctuations in molecular dynamics and normal mode simulations. Proteins: Structure, Function, and Bioinformatics, 1991, 11(3), 205-217. DOI: 10.1002/prot.340110305
[61] Zhu F, Tan C, Li C, Ma S, Wen H, Yang H, et al. Design of a multi-epitope vaccine against six Nocardia species based on reverse vaccinology combined with immunoinformatics. Frontiers in Immunology, 2023, 14, 1100188. DOI: 10.3389/fimmu.2023.1100188
[62] Zhang G, Su Z. Inferences from structural comparison: flexibility, secondary structure wobble and sequence alignment optimization. In: BMC bioinformatics, 2012, 13(Suppl 15), S12. DOI: 10.1186/1471-2105-13-S15-S12
[63] Carugo O, Pongor S. A normalized root-mean-spuare distance for comparing protein three-dimensional structures. Protein Science, 2001, 10(7), 1470-1473. DOI: 10.1110/ps.690101
[64] Ayaz H, Suleman M, Shah AA, Abideen SA, Ahmad F, Ali M, et al. Molecular modeling to design a multiepitope vaccine against emerging tick-borne Yezo virus and its validation through biophysics techniques. *In Silico* Pharmacology, 2025, 13(2), 80. DOI: 10.1007/s40203-025-00370-0
[65] Morita K, Tachikawa N, Matsuda T, Goto A, Matsuyama H, Mitsuhashi K, et al. A Case of co-infection with Yezo virus and borrelia miyamotoi. Journal of Hospital General Medicine, 2025, 7(3), 92-95. DOI: 10.60227/jhgmeibun.2024-0030
[66] Sunita, Singhvi N, Singh Y, Shukla P. Computational approaches in epitope design using DNA binding proteins as vaccine candidate in Mycobacterium tuberculosis. Infection, Genetics and Evolution, 2020, 83, 104357. DOI: 10.1016/j.meegid.2020.104357
[67] Oyarzun P, Kobe B. Computer-aided design of T cell epitope-based vaccines: Addressing population coverage. International Journal of Immunogenetics, 2015, 42(5), 313-321. DOI: 10.1111/iji.12214
[68] Kim HJ, Kim JK, Seo SB, Lee HJ, Kim HJ. Intranasal vaccination with peptides and cholera toxin subunit B as adjuvant to enhance mucosal and systemic immunity to respiratory syncytial virus. Archives of Pharmacal Research, 2007, 30(3), 366-371. DOI: 10.1007/BF02977620
[69] Kar T, Narsaria U, Basak S, Deb D, Castiglione F, Mueller DM, et al. A candidate multi-epitope vaccine against SARS-CoV-2. Scientific Reports, 2020, 10(1), 10895. DOI: 10.1038/s41598-020-67749-1
[70] Sauer K, Harris T. An effective COVID-19 vaccine needs to engage T cells. Frontiers in Immunology, 2020, 11, 581807. DOI: 10.3389/fimmu.2020.581807
[71] Yao R, Xie C, Xia X. Recent progress in mRNA cancer vaccines. Human Vaccines & Immunotherapeutics, 2024, 20(1), 2307187. DOI: 10.1080/21645515.2024.2307187
[72] Pardi N, Krammer F. mRNA vaccines for infectious diseases-advances, challenges and opportunities. Nature Reviews Drug Discovery, 2024, 23(11), 838-861. DOI: 10.1038/s41573-024-01042-y
[73] Shi J, Zhu Y, Yin Z, He Y, Li Y, Haimiti G, et al. *In silico* designed novel multi-epitope mRNA vaccines against Brucella by targeting extracellular protein BtuB and LptD. Scientific Reports, 2024, 14(1), 7278. DOI: 10.1038/s41598-024-57793-6
[74] Dinh P, Tran C, Dinh T, Ali A, Pan S. Hsa_circRNA_0000284 acts as a ceRNA to participate in coronary heart disease progression by sponging miRNA-338-3p via regulating the expression of *ETS1*. Journal of Biomolecular Structure and Dynamics, 2024, 42(10), 5114-5127. DOI: 10.1080/07391102.2023.2225109
[75] Liu WL, Kampouri E, Bui JK, Sekhon MK, Tercero A, Finlay D, et al. Off-the-shelf allogeneic natural killer cells for the treatment of COVID-19. Molecular Therapy-Methods & Clinical Development, 2024, 32(4), 101361. DOI: 10.1016/j.omtm.2024.101361